Analyst

ROYAL SOCIETY OF CHEMISTRY

PAPER

View Article Online
View Journal | View Issue

Cite this: *Analyst*, 2024, **149**, 1609

Toward chemical recycling of PU foams: study of the main purification options†

Eleonora Conterosito, *[a] Marco Monti, [b] Maria Teresa Scrivani,[b] Irene Kociolek,[b] Ilaria Poncini,[b] Chiara Ivaldi, [a] Michele Laus [c] and Valentina Gianotti [a]

Received 3rd November 2023,
Accepted 23rd January 2024

DOI: 10.1039/d3an01909h

rsc.li/analyst

The recovery of the polyol component, after glycolysis of polyurethane (PU) foams coming from automotive waste, was investigated. Several separation methods such as simple sedimentation, centrifugation and liquid–liquid extraction, eventually preceded by an acid washing step, were tested. The obtained fractions were characterized by infrared spectroscopy and CHN elemental analysis. Furthermore, multivariate data analysis was carried out on the infrared spectra by principal component analysis to classify the fractions based on purity. IR spectroscopy coupled with principal component analysis was able to estimate the success of the separation and eventual culprits such as contaminations, which were then quantified by CHN elemental analysis. This approach addresses some critical limitations associated with classical analytical techniques such as NMR, TGA, GPC, MALDI-TOF that often require an extremely accurate separation of the depolymerized product fractions. Moreover, IR spectroscopy and CHN elemental analysis techniques are cheap and widespread in standard materials science laboratories. At last, based on the results of the analysis of the regenerated polyol fractions, and on the foaming tests, considerations were made to guide the choice of the purification method according to the application specifications and greenness.

Introduction

In the last decades, polyurethane (PU) foams have been widely used due to their low density and mechanical strength[1] for a variety of applications such as thermal and acoustic insulation, cushioning, coatings, and sealants. In Europe, PUs ranked as the fifth most employed polymers in 2021, with an annual demand of 4.1 million tons, out of the overall polymer demand of 50.3 million tons.[2] As the use of PUs increases, their end-of-life management has become an urgent issue.[3] In this context, mechanical recycling can be successfully applied to thermoplastic PUs. However, this approach is not suitable for thermosetting PUs, which represent approximately the 80% of the PU industry.[1,4] Therefore, for these materials, chemical recycling by depolymerization and the recovery of the polyol fraction becomes necessary.

Among the various depolymerization processes, which include hydrolysis, aminolysis, and acidolysis,[5] glycolysis stands out prominently due to its high yield performance.[6] The reaction consists in a transesterification between the polyurethane group and a wide excess of low molecular weight glycol, as reported in Scheme 1.[3,7]

At the end of the reaction, a complex mixture of products is obtained, depending on the structure of the starting PU and the nature and amount of the employed glycol. Furthermore, the process can be either a single-phase or a split-phase glycolysis, with the latter yielding the recovered polyol in the upper phase and residues, such as amides and the partially glycolyzed fraction, mainly in the lower phase.[6,8,9] In general, the split-phase process could be preferred because the physical separation leads to higher amounts of recovered products and improved polyol purity.[3,6,10] Additionally, the use of a substantial excess of the glycolysis agent was found to further promote the phase separation,[11] with the glycol acting also as solvent. However, side products coming from glycolysis and some residual glycol can be present in the upper phase, thus interfering with the selectivity of the depolymerization process[7,12] and decreasing the quality of the obtained polyol.

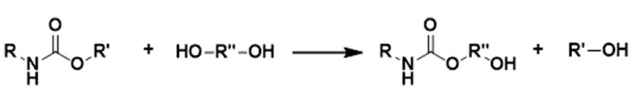

Scheme 1 General scheme of PU glycolysis.

[a]*Dipartimento per lo Sviluppo Sostenibile e la Transizione Ecologica (DiSSTE) Università del Piemonte Orientale, P.zza Sant'Eusebio 5, 13100 Vercelli (VC), Italy. E-mail: eleonora.conterosito@uniupo.it*
[b]*Proplast, Via Roberto di Ferro 86, 15122 Alessandria (AL), Italy*
[c]*Dipartimento di Scienze e Innovazione Tecnologica (DiSIT) Università del Piemonte Orientale, Via T. Michel 11, 15121 Alessandria (AL), Italy*

†Electronic supplementary information (ESI) available: Reactor scheme and picture, complete PCA plots. See DOI: https://doi.org/10.1039/d3an01909h

Among the various glycols, diethylene glycol (DEG) is widely employed for its low cost, good performance in glycolysis reactions[7,9,10,13] and efficiency in the final phase separation.[10] Various catalysts[14] were also used, such as zinc acetate ($ZnAc_2$).

Although glycolysis remains one of the most established methods for the recovery of the polyol from PU, there are still some issues that require improvements to make this process more effective. Firstly, predicting the composition of the post glycolysis mixture, and consequently, the properties of PU foams produced using not-purified polyol,[12] is significantly challenging. Secondly, since the polyol and other glycolysis products (amides, amines, oligomers, and residual glycol) are polar compounds, the separation and purification of the polyol requires a careful optimization. Unfortunately, only a few literature studies, focused on the performances of different purification techniques, are available.[15,16] To address this point, this paper deals with the performances of several purification procedures of the glycolysis products obtained by reacting a polyurethane foam with DEG. The tested purification approaches include both simple methods, as sedimentation and centrifugation, and more complex ones consisting of liquid/liquid extraction, with or without an acidic washing step. To be closer to a real recycling case, the PU foam waste chosen for the study is an automotive post-consumer scrap of unknown composition. Therefore, a preliminary analysis was carried out to characterize the starting material. The composition of the fractions, obtained by different purification methods, was investigated using FT-IR spectroscopy and CHN elemental analysis. Moreover, to determine the most convenient purification method, the maximum amount of information was extracted by the principal component analysis (PCA) multivariate method.[17] Finally, polyol mixtures consisting of a virgin industrial polyol, and the regenerated polyol obtained from the four purification methods, were employed to obtain PU foams.

Experimental

Materials

The starting PU foam (marked PUF) is a post-consumer waste (car top padding). Diethylene glycol (DEG) (ReagentPlus, purity 99%), zinc acetate ($ZnAc_2$) (99.99%), and dichloromethane (DCM) (≥99.9% GC grade, ACS reagent) were purchased from Merck Life Science S.r.l. (Milan, Italy).

The polyurethane system used for the regeneration test is the Huntsman Tecnothane Tecnocell 2, consisting of a polyol blend (RF203/2) and a pre-polymer (MDE300), and kindly supplied by Huntsman. A commercial polyol, Elastoflex E3943/129 specifically employed for the preparation of PU foams for the automotive marked was obtained by BASF (Villanova d'Asti (AT), Italy) and is marked VP along the text.

Methods

Depolymerization. The glycolysis reaction was carried out in a jacketed 1 dm^3 flask equipped with a stirrer and a refluxing condenser as shown in Fig. S1,† under nitrogen atmosphere to avoid oxidation, based on the method described by Wu *et al.*[15] To facilitate the addition of the polyurethane to the reactor, the volume of the foam was reduced by pressing it at 30 bars and 60 °C in a DGTS (Veduggio con Colzano (MB), Italy) P7-34-C press for 5 min. The foam was then cut into pieces of approximately 10 × 10 × 1 mm and reacted in a 1 : 4 mass ratio with DEG, in the presence of $ZnAc_2$ as catalyst,[14] with a mass ratio of $ZnAc_2$/PUF 1 : 100 at 200 °C for 4 hours. The solubility of the polyol in DEG and in ethylene glycol (EG) was tested preliminarily using the pure solvents and their mixtures in different ratios. Pure DEG was chosen since it gave the best phase separation. PUF/DEG mixing ratios of 1 : 1, 1 : 2 and 1 : 3 were also investigated but the high viscosity of the resulting solutions hampered the subsequent purification steps.

Purification. Four different methods to purify the polyol after the glycolysis process were investigated. The first purification method was simple sedimentation. The reaction mixture was left to settle for a week. The upper and the lower phases were then collected and analyzed. The second one consisted in the centrifugation of the raw glycolysis product at 3000 rpm with a Thermo-Fisher (Fisher Scientific Italia, Segrate (MI), Italy) IEC CL31R multispeed centrifuge for 20 min. The upper and the lower phases were then separated using a separating funnel and analyzed.

A liquid/liquid extraction with demineralized water and dichloromethane (DCM) was carried out as third purification method. The extraction was performed in a separating funnel, with a water/DCM/glycolysis product ratio of 1 : 1 : 1 by weight. In the fourth method, the reaction mixture was treated with a 1 M solution of HCl in a weight ratio of 1 : 1 for 10 min at 70 °C, as reported in literature by Simón *et al.*[8] and Molero *et al.*[16] Then, the mixture was extracted with DCM in a 2 : 1 ratio. Table 1 reports the different purification methods and the corresponding sample codes.

Table 1 Purification method and corresponding sample codes

Purification method	Method description	Fraction codes
Gravity separation	The reaction mix is left to settle, upper and lower phases are formed	NP_{up}/NP_{low}
Centrifugation	The reaction mix is centrifuged, two phases are formed	C_{up}/C_{low}
Liquid/liquid extraction	The reaction mix is mixed with water and DCM, upper (water) and lower (DCM) phases are formed	EX_{up}/EX_{low}
Acid wash + lq/lq extraction	The reaction mix is washed with HCl 1 M (acid wash); the reaction/acid water mix is added with DCM; upper and lower phases are formed	$AW + EX_{up}/AW + EX_{low}$

Refoaming of PU. Refoaming tests were carried out using the Tecnothane Tecnocell (Huntsman Tecnoelastomeri, Castelfranco Emilia (MO), Italy) PU as the base system by substituting the 15% of polyol RF203 with an equivalent amount of polyol recovered from the glycolysis process. The percent composition of the mixture is MDE300 43%, RF203/2 52%, recovered polyol 5%. The prepolymer (MDE300) and the blend of polyols including the polyol recovered from the glycolysis process were vigorously mixed at 40 °C and the foam was extracted after 15 min (cream time 25 s).

Characterization techniques. FT-IR measurements were carried out in transmittance with a PerkinElmer (Milano, Italy) Spectrum 400.

The elemental analysis CHN (carbon, nitrogen and hydrogen) was carried out using an "EA3000" CHN analyzer by EuroVector (Milano, Italy). Reaction tube and GC oven temperatures were 980 °C and 100 °C, respectively. Atropine sulphate was used as calibration standard.

PCA analysis and clustering were performed on the IR spectra using the RootProf software.[18] Some test runs were performed to define the preprocess and the range to be used. The ranges considered for the analysis were 600–1800 cm^{-1} and 2800–3600 cm^{-1}. The spectra were rescaled using a standard normal variate (SNV) procedure. Profiles are rescaled by the following expression:

$$y' = (y - \langle y \rangle)/\sigma,$$

where $\langle y \rangle$ is the average value of the same profile and σ is its standard deviation. In the first run, the IR spectra of the VP, DEG and PUF were given as input for the analysis together with those of the samples. In the second run, discussed in detail in the paper, the PUF spectrum was excluded from the analysis.

Results

Since the PU used for the study is a real post-consumer waste coming from automotive, its composition and precise characteristics are unknown. In all cases when the formulation is not prepared by mixing all the individual ingredients, a two-component system is employed for the industrial-scale production of PU foams. The first component mainly comprises the polyol blend and additives, while the second component contains the isocyanate functions included in a prepolymer structure.[19] A characterization by FT-IR of PUF was performed to gather as much information as possible about its structure.

Spectroscopic characterization of the starting materials

The FT-IR spectrum of PUF (Fig. 1, black curve) exhibits a large band in the 3450–3300 cm^{-1} that can be attributed to the stretching of NH groups of urethanes (grey region). Generally, free NH stretching band, NH groups hydrogen bonded with urethane carbonyl oxygens and/or ether oxygens are observed at 3450, 3350–3300 and 3310–3290 cm^{-1}.[20] Hence, signals in PUF spectrum observed at 3340 and 3292 cm^{-1} confirm the

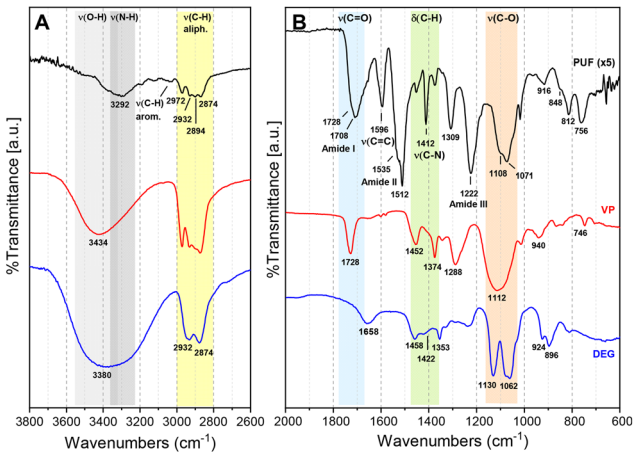

Fig. 1 FT-IR spectra of PU (black curve, intensity multiplied per 5), VP (red curve) and DEG (blue curve), intensity multiplied per (5) in the (A) high frequency and (B) low frequency range.

presence of hydrogen bond between PUF chains. Aromatic and aliphatic C–H stretching modes are detected in the 3100–3000 and 3000–2800 cm^{-1} spectral ranges, respectively, the former with a lower intensity, as expected. Particularly, signals at 2972 and 2894 cm^{-1} are attributed to the asymmetric and symmetric stretching modes of methyl groups, while bands at 2932 and 2874 cm^{-1} are related to the asymmetric and symmetric stretching modes of methylene groups (yellow region). The strong and complex band from 1620 to 1760 cm^{-1} is ascribable to the amide l mode and, in general, to C═O stretching vibrations.[21] Interpreting this adsorption is challenging since it is composed by several individual signals, and it is also influenced by the presence of hydrogen bonds. Specifically, the carbonyl signal of H-bonded groups can be detected at lower wavenumbers (around 1700 cm^{-1}), whereas non H-bonded groups are associated to bands at higher wavenumbers (1728 cm^{-1}).[22] In addition, other components can contribute to this broad band, notably the C═O stretching modes of ester groups in the polyol (1730 cm^{-1}) and the C═O stretching vibration of the isocyanurate rings (1708 cm^{-1}), a product of isocyanate trimerization. The isocyanurate ring is also responsible for the absorption at 1412 cm^{-1}, attributed to its C–N stretching.[23] Urethane groups are also related to two strong and large absorptions, due to the in-phase combination of N–H in plane bending and C–N stretching vibrations, the amide II band (δ(N–H) + ν(C–N)) at 1512 cm^{-1} and amide band III (ν(C–N) + δ(N–H)) at 1222 cm^{-1}. Similarly to amide mode I, amide II absorption is sensitive to hydrogen bonding, with signal at 1535 cm^{-1} assigned to H-bonded N–H vibration between N–H and C═O groups and band at 1512 cm^{-1} attributed to free N–H groups.[24] Additionally, C–O–C stretching mode is detected at 1072 cm^{-1}, whereas the shoulder at 1108 cm^{-1} is attributed to the asymmetric stretching of the ether group of the glycol. At last, the in plane aromatic C═C stretching mode, arising from the isocyanate component, is observed at 1596 cm^{-1}.

Exploiting knowledge about common industrial polyol foam systems composition and the FT-IR spectral features of PUF, the polyol blend best matching PUF was identified as Elastoflex E3943/129 (BASF). The spectrum of Elastoflex E3943/129, labeled as VP, is reported in Fig. 1 (red curve) for comparison. Furthermore, in the high frequency region of the VP spectrum, a broad signal due to OH stretching centered at 3434 cm^{-1} is detected. As per PUF, characteristic signals arising from both methyl and methylene groups are clearly visible in the 3000–2800 cm^{-1} spectral range (light grey region). Moreover, a strong absorption at 1728 cm^{-1} assigned to C=O stretching of ester groups of the polyol (light blue region), bands related to bending of alkane C–H groups are observed at 1452 and 1374 cm^{-1} (green region), as well as C–O vibrations from ester, ether and hydroxyl groups are detected in the 1030–1288 cm^{-1} region.

The spectrum of DEG is also reported for comparison (Fig. 1, blue curve). A broad absorption related to OH stretching is displayed at 3402 cm^{-1} (light grey region). In the aliphatic C–H stretching modes range (3000–2800 cm^{-1}), only asymmetric and symmetric stretching modes related to methylene groups at 2932 and 2874 cm^{-1} are observed. The band around 1650 cm^{-1} is assigned to the δ(HOH) vibration of the coordinated water. In addition, signals at 1458 and 1353 cm^{-1} are assigned to δ(C–H) of alkane chains (green region), the weak band at 1422 cm^{-1} is attributed to C–O–H bending, while the band at 1130 cm^{-1} to asymmetric C–O–C stretching and the absorption at 1062 cm^{-1} to asymmetric C–C–OH stretching (orange region). The shape of the C–O stretching bands at 1130 and 1062 cm^{-1} is typical of DEG and will be used for its identification.

Glycolysis product characterization

According to the IR characterization, several functional groups are present in the polyurethane foam, including ester groups coming from the polyol, urethane groups from the main reaction between isocyanates and the hydroxy groups of the polyol, and ureic groups deriving from the reaction between isocyanates and the amines that are in turn the products of the reaction between isocyanates and water. Therefore, the chemolytic process carried out using a large excess of ethylene glycol could lead to oligomers containing a plethora of functional groups. Hydroxy groups are the main terminal groups but also amino groups can be present not only as terminal groups but also along the main chain due to the occurrence of decarboxylation reactions. Depending on the molecular weight, all these oligomers could be insoluble and therefore included in the solid fraction or solubilized in glycol.

As previously described, after PU glycolysis, four different polyol separation methods were explored: sedimentation, centrifugation, and liquid–liquid extraction with and without acidic washing pretreatment (Table 1). Sedimentation is the easiest and cost-effective purification method, resulting in an upper brownish phase (NP_{up}) and a lower yellowish phase (NP_{low}) centrifugation allowed achieving a faster separation, leading to upper brownish phase (C_{up}) and a lower yellowish phase (C_{low}) as per sedimentation method. Both methods should separate the oligomers, precipitated in the solid phase, from the polyol, that should be found in the upper phase.

For liquid–liquid extraction, a DCM/water mixture was chosen, since DCM is a suitable solvent for polyol, and water for DEG. Whether using method with (AW + EX) or without (EX) acidic pretreatment, a brownish lower fraction (AW + EX_{low} or EX_{low}) in DCM and a yellowish upper fraction (AW + EX_{up} or EX_{up}) in water were collected. Extraction with one solvent similar to polyol and one similar to DEG, should enhance the polyol purification from the residual DEG and more polar residues. The acidification should push the extraction of amine residues even further.

FT-IR characterization of the fractions. FT-IR spectra of all the fractions are reported in Fig. 2, with the previously assigned characteristic signals. In general, significant variations among the samples are observed in the aliphatic CH stretching region between 3000–2800 cm^{-1} (yellow area), in the C–O vibrations spectral range between 1200–1000 cm^{-1} (orange area) and in the fingerprint region between 850 and 950 cm^{-1} (green area). A preliminary analysis and comparison of the spectra in these spectral ranges suggests that DEG is the principal component of the NP_{low}, C_{low}, EX_{up} and AW + EX_{up} fractions (hereafter referred to as DEG-rich fractions). Specifically, in the high frequency region of their spectra, only two bands at 2932 and 2874 cm^{-1}, ascribable to asymmetric and symmetric $\nu(CH_2)$, are observed. Notably, the CH bending of aliphatic chains occurs at 1353 cm^{-1} instead of 1374 cm^{-1}. Furthermore, in the ν(C–O) spectral region, characteristic stretching bands of DEG at 1130 and 1062 cm^{-1} are detected. Lastly, the shape of the spectra in the fingerprint spectral

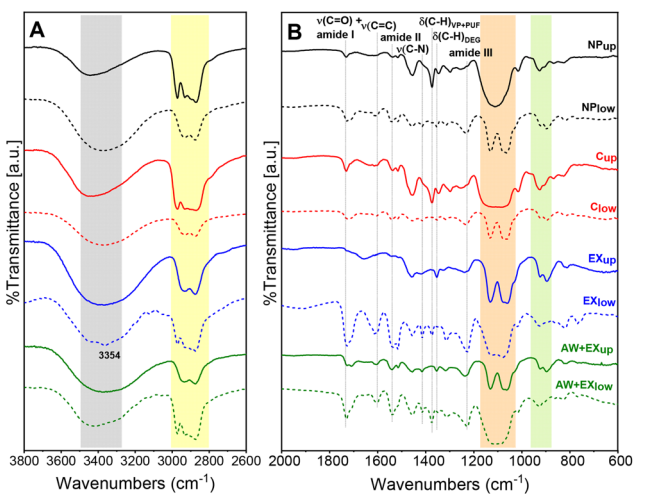

Fig. 2 FT-IR spectra in the (A) high and (B) low frequency region of the upper and lower phases obtained from sedimentation (NP), centrifugation (C), liquid–liquid extraction without (EX) and with (AW + EX) acidic treatment. Significant variations among the samples are observed in the highlighted spectral regions. In grey, NH stretching region. In yellow, aliphatic CH_2 and CH_3 stretching region. In orange, C–O stretching region of ethers, esters, and hydroxyl groups. In green, fingerprint region.

range is similar to the one observed for DEG. It is noteworthy that, among all DEG-rich fractions, EX_{up} exhibits a lower quantity of PUF residues with respect to the other DEG-rich fractions, as confirmed by the lower intensity of amide I, II and III modes, as well as ν(C=C) and ν(C–N) vibrations. In contrast, polyol is mainly found in NP_{up}, C_{up}, EX_{low} and AW + EX_{low} fractions (hereafter named polyol-rich fractions). Notably, in the CH stretching region of the polyol-rich fractions spectra, both asymmetric and symmetric stretching of methyl and methylene groups are detected (yellow area). In addition, a broad signal centered at 1112 cm^{-1} is observed in the C–O stretching range (orange area), as the signal displayed by pure VP. Moreover, CH bending of aliphatic chains occurs at 1374 cm^{-1}, as well the overall profile of the spectra in the fingerprint region (green area) resembles the VP and PUF spectra. The relative intensities of principal signals and shape of the C–O broad absorption suggest that the higher concentration of PUF residues is contained in the EX_{low} fraction. Indeed, EX_{low} spectrum exhibits the most prominent intensities of amide I, II and III modes associated with unreacted PUF, together with a signal at 3354 cm^{-1}, ascribable to NH stretching. In addition, the shape of the broad C–O adsorption closely resembles that of PUF. In conclusion, both sedimentation and centrifugation methods result in a biphasic mixture, with DEG mostly concentrated in the lower phase, and polyol and PUF residues in the upper phase. In contrast, for extraction methods, DEG is the main component of the upper phase (water), while polyol is mainly concentrated in the lower phase (DCM). Notably, the absence of the band at 3354 cm^{-1} in the AW + EX_{low} spectrum suggests that the acidic washing provides an efficient extraction in water of the amide-containing residues.

PCA analysis. Due to the complexity of the FT-IR spectra, classification and multivariate methods, such as clustering analysis and principal component analysis (PCA), were applied. In fact, PCA is a useful technique for enhancing the understanding of a complex dataset with numerous variables.[25,26] Formally, PCA reduces the dimensionality of a dataset by substituting the original variables with smaller set of new ones known as principal components (PCs). These new variables are independent and are chosen so that the first PC can be represented by a new axis sitting in the direction of the dataset maximum variance. Then, the second PC is orthogonal to the first one, explaining the maximum amount of the residual variance, and this pattern continues for subsequent PCs. Within our dataset, each fraction is represented by its IR spectrum and is considered as a "sample", with each wavenumber of the spectra represents a variable. The PCA loading plot indicates the correlations between original variables and the PCs, while the score plot represent the projection of each sample in the space of the PCs.

The spectra of all the fractions, together with PUF, DEG and VP spectra as reference samples, were loaded in the Rootprof software. After selecting the spectral range of interest from 600 to 1800 cm^{-1} and from 2800 to 3600 cm^{-1}, a preliminary clustering analysis was performed on the dataset composed of all the normalized IR spectra. This analysis yielded three distinct groups (Fig. S2†), each containing the spectrum of one of the reference samples. Specifically, the first group includes the fractions containing the higher amount of polyol, together with the VP spectrum. The second group consists of the samples in which DEG is predominant, while PUF stands alone in the third group. Therefore, in accordance with a preliminary FT-IR characterization, VP is categorized within the group including the upper phases obtained through sedimentation and centrifugation (NP_{up} and C_{up}), as well as the lower phases resulting from the extraction procedures (EX_{low} and AW + EX_{low}). Such results are coherent with literature studies.[27,28] In fact, after simple sedimentation, the polyol is recovered in the upper phase due to its lower density compared to DEG. In contrast, extraction methods result in polyol being solubilized in the DCM phase (lower phase), according to the higher affinity of polyol for DCM. PCA identified two significant principal components, PC1 and PC2, explaining 96.7% of the overall variance (65.88% by PC1 and 30.78% by PC2).

The PCA score plot of PC1 *vs.* PC2 (Fig. S3†) shows that the three pure phases (DEG, VP and PUF) are well separated. The polyol-rich fractions are clustered at the top, with VP, and the ellipse is stretched towards PUF to include EX_{low}. This suggests that EX_{low} likely contains a higher percentage of PUF residues compared to the other samples in this group. Conversely, all other fractions are grouped with DEG at the bottom left of the score plot.

To gain a deeper insight into the separation from DEG, especially considering that PUF was not grouped with any other sample, clustering analysis was repeated after removing the spectrum of PUF from the dataset. The clustering analysis on the revised dataset once again leads to the separation of the samples into three clusters (Fig. 3). The two groups containing DEG and VP are the same observed in the previous PCA, whereas the other one only includes the EX_{low} sample.

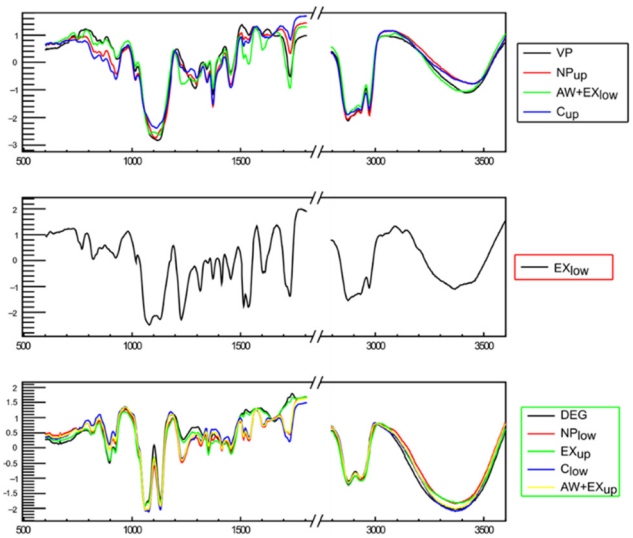

Fig. 3 Clustering of the IR spectra after normalization. The samples are divided into three clusters according to similarities in their IR spectra.

Subsequently, PCA was performed on the same dataset to provide a better analysis of the spectra within each group.

The analysis identified two principal components, PC1 and PC2, explaining 94.4% of the overall variance (75.43% by PC1, 18.97% by PC2). Since the variables in the dataset are the wavenumbers of the spectra, the loading plot of each PC resembles an IR-spectrum, in which the most intense bands represent the most prominent spectroscopic features of samples with high scores on that PC. The score and loading plots of the two PCs are reported for completeness in Fig. S4 and S5.† The loading plot of PC1 *vs.* PC2 comprising all wavenumbers is reported in Fig. S7,† while the loading plot of PC1 *vs*. PC2 for selected wavenumbers is illustrated in Fig. 4A. The bands with higher loadings on the PCs were selected and assigned to polyol, DEG or PUF residues. In particular, the bands at 1374 and 1112 cm^{-1}, which are characteristic of the polyol, and the signals at 1658, 1130 and 1062 cm^{-1}, which are indicative of DEG, were chosen.

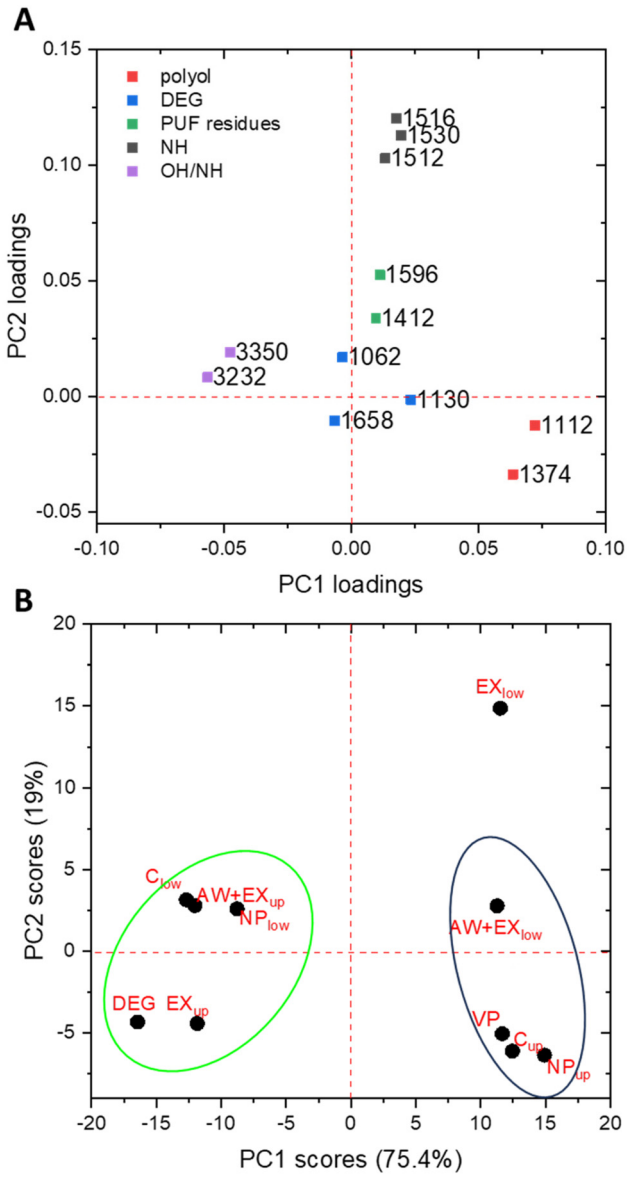

Fig. 4 (A) Loading plot of PC1 *vs.* PC2 for the selected variables (wavenumbers) and (B) score plot of PC1 *vs*. PC2.

Moreover, the bands at 1596 cm^{-1} (aromatic C=C stretching mode) and 1412 cm^{-1} (C–N stretching of the isocyanurate ring) were selected along with those of N–H bending modes (1530, and 1516 cm^{-1}), all of which are indicative of the presence of PUF residues. In Fig. 4A, the wavenumbers attributed to polyol have the highest values on PC1, whereas all other bands are below 0.05 in absolute value. This means that PC1 is mostly correlated to the amount of polyol in the samples. It is worth noting that the signals with the highest negative values are associated to the large absorption attributed to OH and NH stretching. Although this absorption is not specific, its intensity should be higher in DEG-rich and PUF residues-rich samples rather than in polyol-rich fractions. Indeed, on the far-left side of the score plot (Fig. 4B), DEG and DEG-rich fractions are clustered. Concerning PC2, the signals with highest values (Fig. 4A) are those attributed to NH bending modes and associated to PUF residues, while the bands attributed to the aromatic and isocyanurate components of PUF residues are found at lower values. Finally, the signals attributed to DEG are distributed at the lowest values around the intersection of PC1 and PC2, and therefore are not significant.

In the score plot in Fig. 4B, VP is located in the bottom right quadrant, together with C_{up} and NP_{up}. This cluster comprises samples rich in polyol, in accordance with loading plot, where the polyol IR bands exhibit high positive values on PC1 and negative values of PC2. Conversely, DEG and EX_{up} are located at high negative values of PC1, as these samples contain the least amount of polyol and PUF residues. In the top left quadrant, placed in correspondence with the OH/NH signals in the loading plot, C_{low}, AW + EX_{low} and NP_{low} are found. These samples contain a large amount of OH and NH groups (*i.e.*, high amounts of both DEG and PUF residues). Furthermore, EX_{low} is placed at high values on both PC1 and PC2, suggesting that it contains a substantial amount of polyol as well as significant PUF residues, but a low amount of DEG. Accordingly, the fractions with high polyol content and low amount of DEG and PUF residues are C_{up}, NP_{up}, and AW + EX_{low}.

Elemental analysis (CHN) and refoaming tests. Elemental CHN analysis was conducted on the polyol-rich phases, using the percent of nitrogen (%N) as a quantitative indicator to evaluate the efficiency of PUF residue separation from the polyol phases. This approach relies on the assumption that nitrogen should exclusively originate from the isocyanate component, and the recovered polyol should ideally contain none. Consequently, a low %N value indicates a good separation of PUF residues from the polyol. Experimental results of CHN analysis are reported in Table 2. Samples C_{up} and NP_{up} exhibit the lowest %N values, suggesting that density-based separation methods are the most efficient in eliminating PUF residues. In contrast, the EX_{low} fraction shows the highest %N, confirming that the extraction method without acidic treatment co-extracts

Table 2 Results of the CHN elemental analysis on the starting materials and on the samples

Sample	N%	C%	H%
PUF	7.63 ± 0.03	67.8 ± 0.1	6.6 ± 0.1
VP	0.30 ± 0.06	54.8 ± 0.7	9.5 ± 0.2
NP_{up}	0.7 ± 0.1	57.1 ± 0.7	9.97 ± 0.06
C_{up}	0.50 ± 0.02	58.0 ± 0.2	10.09 ± 0.05
EX_{low}	4.26 ± 0.05	60.49 ± 0.07	8.42 ± 0.03
AW + EX_{low}	1.32 ± 0.03	55.6 ± 0.8	9.4 ± 0.1

some nitrogen-containing compounds. Notably, the use of acid pretreatment results in AW + EX_{low} sample displaying a lower %N than EX_{low}.

At last, to evaluate the applicability of the recovered polyol obtained from the different purification methods, some foaming tests were carried out. Fig. 5 reports, as typical examples, images of foams obtained by substituting 15% of the RF203/2 component of the Tecnothane Tecnocell system with the fractions NP_{up}, C_{up}, EX_{low}, and AW + EX_{low} together with a reference sample obtained using pure RF203/2. All foams were prepared using the same formulation for comparison. In this way the resulting foam is also affected by the amount of residual DEG, being itself a short chain polyol. The foam obtained from AW + EX_{low} shows the best quality among the four samples containing the recovered polyol whereas the use of NP_{up} leads to an inferior quality product. In the foam obtained using EX_{low}, the yellowish colour evidences the presence of amines. Although the separation from depolymerization residues is better in NP_{up} than in AW + EX_{low}, the larger amount of residual DEG in NP_{up} is particularly detrimental to the foaming process. Similar foams can be prepared using up to 30% of AW + EX_{low}.

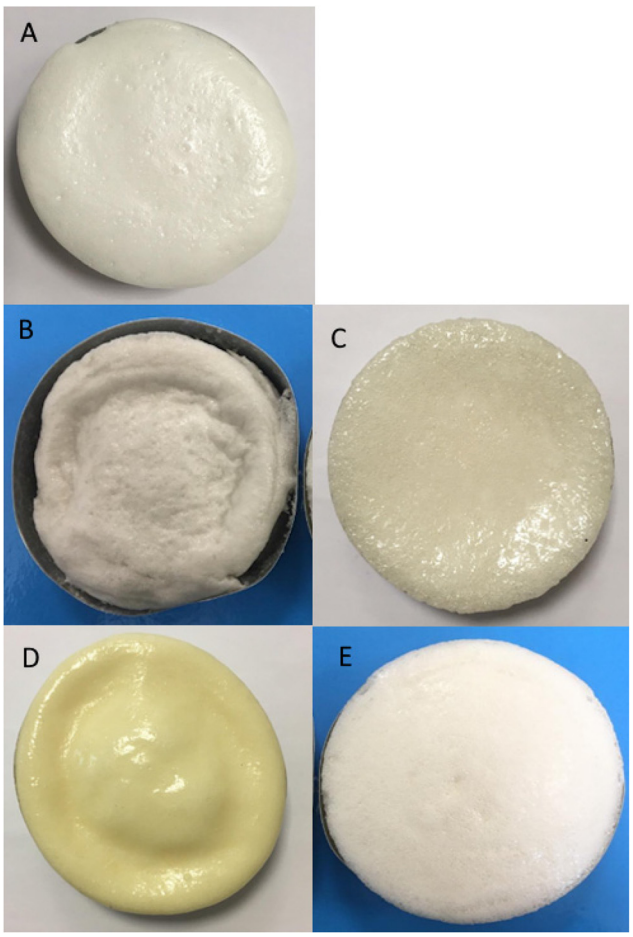

Fig. 5 Foaming test results using (A) VP, (B) NP_{up}, (C) C_{up}, (D) EX_{low} and (E) AW + EX_{low} fractions.

Discussion

From the viewpoint of sustainability of the separation process, a simple sedimentation allows the recovery of a sufficient amount of polyol, albeit with some residual DEG, while avoiding the use of dichloromethane, needed to perform an extraction step. Conversely, extraction procedures offer a better separation from DEG and higher polyol recovery, but they require an acidic pretreatment and the use of organic solvents. Therefore, the choice of the separation method should be made according to the desired product specifications. For low-demanding applications, sedimentation represents a viable and greener approach, while for applications requiring higher loading or greater purity of the initial polyol, extraction methods should be preferred. These considerations are important in the perspective of future scale-up and industrial implementation. As a result, the proposed approach offers broad applicability, cost-effectiveness, and environmental sus-

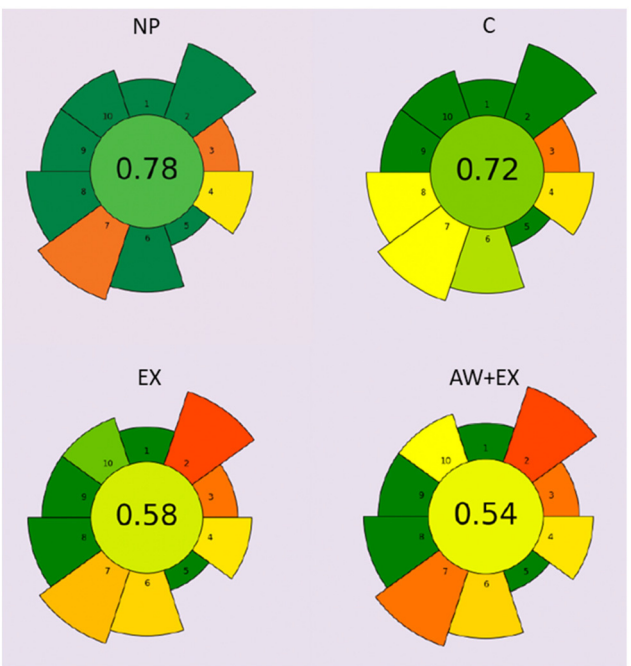

Fig. 6 AGREEprep analysis results.

tainability. With the aim of evaluating greenness in a more quantitative way, different analytical green metrics approaches found in the literature were applied, but they are all designed for sample preparation methods in view of instrumental analysis, and therefore not very appropriate in our case. The most suitable one was found to be the AGREEprep[29] approach. Ten aspects of preparation are evaluated with objective data to which the researcher associates a subjective weight (details reported in Table S1†). To effectively compare the four procedures, the relative weights of the ten parameters were always set equal. In Fig. 6 the resulting schemes are reported. In the center there are the cumulative scores, confirming that simple sedimentation is the greenest approach but also evidencing that also the other approaches obtain sufficient scores. The culprits of these techniques are the power consumption of centrifugation, and the use of hazardous chemicals such as dichloromethane and hydrochloric acid for the extraction procedures.

Conclusions

The present work represents a systematizing study for the development of methods for recycling, recovering and reusing PU waste materials. The efficiency of these processes requires in fact, integrated analytical methods for the characterization of the produced fractions. However, accurate development and validation of the method proposed are often lacking in the fields of materials and polymers. The depolymerization of post-consumer PU foam was selected as a means to replicate a real-world scenario when dealing with waste material recycling. The spectroscopic approach aided by multivariate data analysis, proved to be effective, and is easy to implement in an industrial framework. This method could also be applied to other similar situations, where the recovery of a species of interest from waste materials with unknown composition is required. IR spectroscopy, coupled with principal component analysis, was able, alone, to estimate the success of the separation and eventual culprits such as contaminations, which were then quantified by CHN elemental analysis. This approach addresses some critical limitations associated with classical analytical techniques employed in the field of material science, such as NMR, TGA, GPC, MALDI-TOF that often require an extremely accurate separation of the depolymerized product fractions. Moreover, IR spectroscopy and CHN elemental analysis are cheap and widespread techniques in standard materials science laboratories. At last, based on the results of the analysis of the regenerated polyol fractions, and on the foaming tests, considerations were made to guide the choice of the purification method according to the application specifications and greenness.

Conflicts of interest

There are no conflicts to declare.

Author contributions

Conceptualization: E. C., M. M., M. S., C. I., V. G., M. L. Data curation: E. C., M. M. Formal analysis, E. C., C. I., V. G., M. S. Funding acquisition: M. M., M. S., M. L. Investigation: I. K., I. P. Resources: M. M., M. S., V. G., M. L. Supervision: V. G., M. L. Visualization: E. C., C. I., I. K. Writing – original draft: E. C., M. M., M. S., I. K., V. G. Writing – review and editing: E. C., C. I., V. G., M. L.

Acknowledgements

This research was funded by European regional Development Funding Programme managed by Italian Piedmont Region (POR-FESR 2014-2020) (Reciplast Project).

References

1 S.-R. Shin, H.-N. Kim, J.-Y. Liang, S.-H. Lee and D.-S. Lee, *J. Appl. Polym. Sci.*, 2019, **136**, 47916.
2 Plastics - the Facts 2022·Plastics Europe, **https://plasticseurope.org/knowledge-hub/plastics-the-facts-2022-2/**, (accessed 16 March 2023).
3 W. Yang, Q. Dong, S. Liu, H. Xie, L. Liu and J. Li, *Procedia Environ. Sci.*, 2012, **16**, 167–175.
4 D. Allan, J. H. Daly and J. J. Liggat, *Polym. Degrad. Stab.*, 2019, **161**, 57–73.
5 K. M. Zia, H. N. Bhatti and I. A. Bhatti, *React. Funct. Polym.*, 2007, **67**, 675–692.
6 P. Zahedifar, L. Pazdur, C. M. L. Vande Velde and P. Billen, *Sustainability*, 2021, **13**, 3583.
7 P. Zhu, Z. B. Cao, Y. Chen, X. J. Zhang, G. R. Qian, Y. L. Chu and M. Zhou, *Environ. Technol.*, 2014, **35**, 2676–2684.
8 D. Simón, A. M. Borreguero, A. de Lucas and J. F. Rodríguez, *Polym. Degrad. Stab.*, 2015, **121**, 126–136.
9 D. Simón, A. M. Borreguero, A. de Lucas and J. F. Rodríguez, *Polym. Degrad. Stab.*, 2014, **109**, 115–121.
10 C. Molero, A. de Lucas and J. F. Rodríguez, *Polym. Degrad. Stab.*, 2006, **91**, 221–228.
11 M. M. A. Nikje and F. H. A. Mohammadi, *Polym.-Plast. Technol. Eng.*, 2010, **49**, 818–821.
12 J. Braslaw and J. L. Gerlock, *Ind. Eng. Chem. Process Des. Dev.*, 1984, **23**, 552–557.
13 R. Heiran, A. Ghaderian, A. Reghunadhan, F. Sedaghati, S. Thomas and A. H. Haghighi, *J. Polym. Res.*, 2021, **28**, 22.
14 L. M. Dos santos, C. L. P. Carone, J. Dullius and S. Einloft, *Polim.: Cienc. Tecnol.*, 2013, **23**, 608–613.
15 C.-H. Wu, C.-Y. Chang, C.-M. Cheng and H.-C. Huang, *Polym. Degrad. Stab.*, 2003, **80**, 103–111.
16 C. Molero, A. de Lucas and J. F. Rodríguez, *Solvent Extr. Ion Exch.*, 2006, **24**, 719–730.

17 M. Monti, E. Perin, E. Conterosito, U. Romagnolli, B. Muscato, M. Girotto, M. T. Scrivani and V. Gianotti, *Resour., Conserv. Recycl.*, 2023, **188**, 106691.
18 R. Caliandro and D. B. Belviso, *J. Appl. Crystallogr.*, 2014, **47**, 1087–1096.
19 F. M. de Souza, P. K. Kahol and R. K. Gupta, in *Polyurethane Chemistry: Renewable Polyols and Isocyanates*, American Chemical Society, 2021, vol. 1380, pp. 1–24.
20 K. Kojio, S. Nakashima and M. Furukawa, *Polymer*, 2007, **48**, 997–1004.
21 R. D. Priester, J. V. Mcclusky, R. E. O'Neill, R. B. Turner, M. A. Harthcock and B. L. Davis, *J. Cell. Plast.*, 1990, **26**, 346–367.
22 J. Bandekar and S. Klima, *J. Mol. Struct.*, 1991, **263**, 45–57.
23 J. Reignier, F. Méchin and A. Sarbu, *Polym. Test.*, 2021, **93**, 106972.
24 F. C. Wang, M. Feve, T. M. Lam and J.-P. Pascault, *J. Polym. Sci., Part B: Polym. Phys.*, 1994, **32**, 1305–1313.
25 R. Caliandro, V. Toson, L. Palin, E. Conterosito, M. Aceto, V. Gianotti, E. Boccaleri, E. Dooryhee and M. Milanesio, *Chem. – Eur. J.*, 2019, **25**, 11503–11511.
26 E. Conterosito, M. Milanesio, L. Palin and V. Gianotti, *RSC Adv.*, 2016, **6**, 108431.
27 C. Molero, A. de Lucas, F. Romero and J. F. Rodríguez, *J. Appl. Polym. Sci.*, 2008, **109**, 617–626.
28 X. Wang, H. Chen, C. Chen and H. Li, *Fibers Polym.*, 2011, **12**, 857–863.
29 W. Wojnowski, M. Tobiszewski, F. Pena-Pereira and E. Psillakis, *TrAC, Trends Anal. Chem.*, 2022, **149**, 116553.